Visual Analysis of Polarization Domains
in Barium Titanate during Phase Transitions

Tobias Brix   Florian Lindemann   Jörg-Stefan Praßni   Stefan Diepenbrock   Klaus Hinrichs

University of Münster
Einsteinstraße 62
Germany 48149, Münster, NRW
t.brix | lindemann | j-s.prassni | diepenbrock | khh @uni-muenster.de

ABSTRACT

In recent years, the characteristics of ferroelectric barium titanate ($BaTiO_3$) have been studied extensively in materials science. Barium titanate has been widely used for building transducers, capacitors and, as of late, for memory devices. In this context, a precise understanding of the formation of polarization domains during phase transitions within the material is especially important. Therefore, we propose an application that uses a combination of proven visualization techniques in order to aid physicists in the visual analysis of molecular dynamic simulations of $BaTiO_3$. A set of linked 2D and 3D views conveys an overview of the evolution of dipole moments over time by visualizing single time steps as well as combining multiple time steps in one single static image using flow radar glyphs. In addition, our system semi-automatically detects polarization domains, whose spatial relation can be interactively analyzed at different levels of detail on commodity hardware. The evolution of selected polarization domains over their lifetime can be observed by a combination of animated spatial and quantitative views.

Keywords

Visualization in Physical Sciences and Engineering, Glyph-based Techniques, Time-varying Data.

1   INTRODUCTION

Since ferroelectricity in barium titanate ($BaTiO_3$) has been discovered in 1945 by Wul and Goldman [25], it has been one of the most exhaustively studied materials [15]. It has an industrial importance based on the common usage of $BaTiO_3$ in thin films ([21],[5]) for memory devices like Fe-RAM.

From a physical point of view, the material is interesting because of its displacive phase transitions and its polarization domain formation. The movement of positively and negatively charged ions during a phase transition results in local dipole moments in the unit cells of the barium titanate grid. Regions with similarly directed dipole moments are called polarization domains.

A visualization of the evolution of these polarization domains during phase transitions in ferroelectric materials can be useful to get deeper insights into the physical phenomenon of ferroelectricity. In 1963, first approaches relied solely on microscopes [2] to catch a glimpse of domain formation.

As computer simulations of molecular dynamics (MD) have become standard in physical research, the need for a visualization of MD became apparent. Now there exist many software packages for visualizing molecular structures. However, to our knowledge there is no dedicated tool to guide scientists in detecting and exploring ferroelectric domains in a simulation dataset.

In 2012 the topic was even in the focus of the IEEE VisWeek SciVis contest [23]. In this paper we present our application to visualize polarization domains in barium titanate during phase transitions in combination with semi-automatic algorithms to classify domains. The tool provides numerical methods for dipole moment calculation and detection of resulting polarization domains. The user can obtain a quick overview of the behavior of $BaTiO_3$ during phase transitions by using glyph techniques to reduce the potential clutter. A more in-depth study of spatial and temporal evolution of polarization domains is supported by several linked views using proven visualization techniques for a visual analysis, and by numerical parameters and histograms referring to selected time steps or domains for a quantitative analysis. Our application has been implemented in the framework Voreen (Volume Rendering Engine) [18] developed at the University of Münster. All statements according to frames per seconds (fps) or processing times refer to a commodity computer with an Intel i7 processor, 16 GB RAM and an AMD Radeon HD 7900 Series graphics card.

2 RELATED WORK

In the late 1950s theoretical physics conceived the idea of simulating molecular behavior (molecular dynamics) [1] in addition to the observation of molecular phenomena in laboratories with technical devices. With more powerful computers these simulations became more feasible and cost-efficient than laboratory studies. In order to handle the generated simulation data efficiently, numerous molecule representations have been implemented in different software frameworks. Examples of such software frameworks are Visual Molecule Dynamics (VMD) [9] and the Open Visualization Tool OVITO [22] both of which inspired our design.

Although many different representations of molecule structures are frequently employed, like ribbons [3], which usually represent the backbone of protein structures, or Van der Waals surfaces [24], which visualize the surface of a molecule based on the van der Waals forces, we simply use the classic ball-and-stick model by A. Hofmann [10]. Since our application is intended for exploring ferroelectric domains, we do not see a benefit of supporting further molecular representations. If a need for further representations arises we refer to the above mentioned visualization frameworks.

The biggest challenge in molecular visualization is the large quantity of atoms. To visualize millions of atoms at interactive frame rates, advanced rendering algorithms and storage techniques have to be used. Optimized rendering techniques have been presented for example by Lampe et al. [16], who use billboards, i. e., quads facing towards the camera, instead of rendering geometrical spheres for representing the atoms, and by Krone et al. [12], who use a ray casting approach. In our application we employ the billboards as proposed by Lampe et al.

In the past, most visualizations in the physical research of polarization domains in ferroelectric materials have been generated without applying computer rendering techniques. In 1963 Amelinckx and Blank [2] have observed polarization domains in $BaTiO_3$ by an electron microscope and used simple gray scale slices for visualization. Later in 1995, Kolosov et al. [11] visualized ferroelectric domains by an atomic force microscope. Although it has been the first observation with a resolution of 10nm they also used coarse pixelated gray scale slices for visualization. In 2010, Pasćiak et al. [19] employed a 3D approach using an algorithm to automatically detect polarization domains in barium titanate and visualizing the results in a binary volumetric manner by distinguishing unit cells belonging to domains from those which lie outside. In our application we use glyph techniques to represent the domains. We want to stress our use of the flow radar glyph of Hlawatsch et al. [8], which is a glyph based flow visualization applied to a molecular problem. All dipole moments of multiple time steps of the molecular dynamics can be visualized
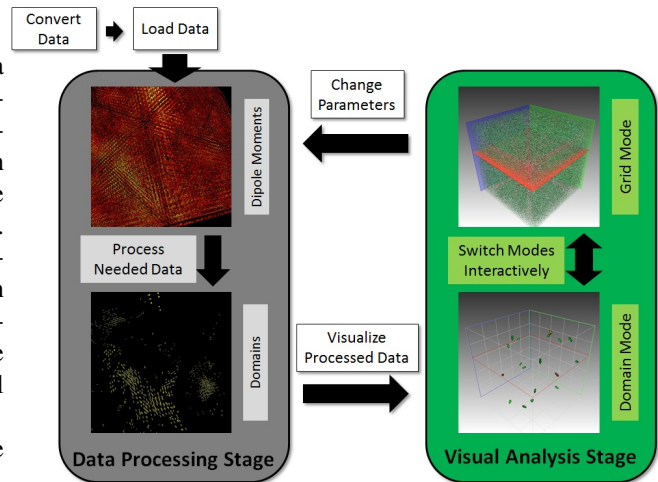

Figure 1: *Schematic representation of the application workflow, which is subdivided in a preprocessing stage and an interactive analysis stage.*

in a single static image by these glyphs.

The application by Scharnowski et al. ([20]) for finding polarization domains and exploring the data in several visualizations was the winning entry in the VisContest 2012 [23]. They used surface representations based on Krone et al. [13] for the polarization domains and vector fields for representing the dipole moments for each unit cell. We are using the same vector visualization for dipole moments, but differ in the domain representation. Furthermore, instead of having only one view to see temporal evolution in the detected polarization domains, which can be tracked and identified over time, we use several linked views to provide an application for supporting physical research in ferroelectrics. One of the latest publications in the field of dipol moment visualizations is from 2012 by Grottel et al.[6], who also use an arrow glyph based representation of the dipol moments. Like Scharnowski et al. they use the framework MegaMol [17] developed at the University of Stuttgart.

3 APPLICATION DESIGN

Our application workflow can be subdivided into two stages as shown in Fig. 1. In the *data processing stage* the dipole moments of each unit cell are computed, and the resulting polarization domains are detected (see Sec. 4). Since these calculations are quite expensive, a diagnosis on the fly is not possible. The subsequent interactive *visual analysis stage* encompasses the visualizations for exploring the data and for analyzing the pre-detected domains (see Sec. 5).

The complete dataset, the precomputed dipole moments and the detected polarization domains are stored in main memory in order to achieve interactive frame rates during the visual analysis stage. Therefore, it is necessary to convert the data obtained from the
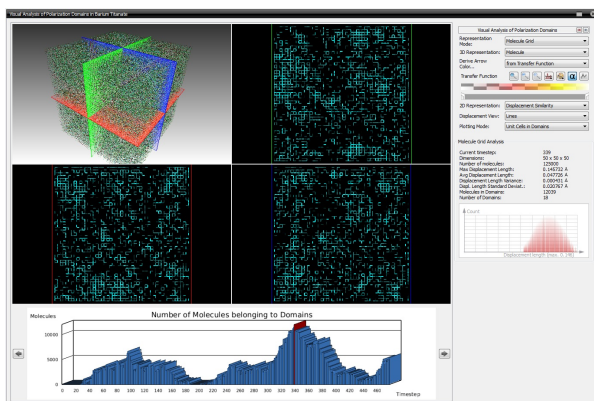
(a) *Layout of the application in grid mode.*
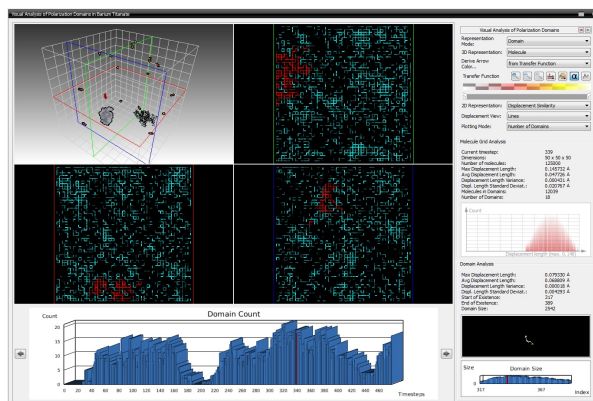
(b) *Layout of the application in domain mode.*

Figure 2: *Example screenshots of the GUI layout in both application modes. Upper/Left: 3D and 2D views. Right: Control menu and statistics. Bottom: Bar plot over all time steps. Lower/Right: radar glyph and domain statistics, only in domain mode.*

molecular dynamics simulation into a binary format to fit into RAM. The dataset contains the positions of $BaTiO_3$ atoms from a 3D unit cell grid over many time steps.

When the atom positions are loaded, the data processing stage can begin with calculating the dipole moment of each unit cell. We provide different methods to accomplish this task, each with different parameters controlled by the user to compensate for inaccuracies caused by the simulation. A detailed description of the methods and our experience is given in Sec. 4.1.

Subsequently the semi-automatic detection of polarization domains can be started, again controlled by the user, who can influence the detection outcome by choosing different methods and parameters (see Sec. 4.2). The domain data contains general information about each domain, like center of mass or average displacement, and a mapping of each unit cell to a unique domain id.

All data structures can be saved and loaded by the application. Hence the results of the data processing stage can be recorded, and if the user resumes data exploration later on the data processing stage can be skipped.

After the data processing stage has finished and the data structures have been stored in main memory, the interactive visual analysis stage can begin. In order to provide the user with a general overview of the full molecule grid as well as specialized views for regions of interest and detected domains, our application allows the user to choose between two different modes, which we call *grid mode* (Sec. 5.1) and *domain mode* (Sec. 5.2). The user can switch between these two modes without noticeable delay. While the display layout is similar in both modes (Fig. 2), grid mode visualizes the entire grid, while domain mode is used to focus on the polarization domains detected by our system. In each mode, three

2D views and one 3D view in the upper left region of the interface allow for a flexible visual analysis of the data. Each view can be focused and enlarged for precise analysis. Each of the 2D views is associated with one of the axis-aligned major planes whose 3D position is marked by color-coded frames in the 3D view (Fig. 2a and 2b upper/left). Additionally, data statistics are displayed on the right side of the interface, depending on the current mode. The user can view time steps by selecting them from the interactive bar plot at the bottom of the system interface by selecting a bar, which directly loads the associated time step, or by using the arrows on both sides of the plot to select the previous or next time step. The plot shows for each time step the total number of unit cells belonging to all identified domains or optionally the number of detected domains in each time step, facilitating the selection of time steps with high domain activity. After selecting an interesting time step, the user can switch to domain mode in order to visualize the domains that have been detected. In this mode, single domains can be interactively selected in the upper left view. For each domain, an individual 3D visualization can be chosen (see Sec. 5.2.1). By using the mentioned left and right arrows next to the bar plot, the user can then view the evolution of a domain over time by stepping through the dataset. Furthermore, in domain mode, the statistics bar will be enlarged to display specific statistics about the selected domain, such as its lifetime or size evolution over time (Fig. 2b lower/right). An extra bar plot shows the number of unit cells belonging to the selected domain highlighting the bar associated to the current time step. A radar glyph (see Sec. 5.1.3) visualizes the average domain dipol moment direction with the same perspective as the actual 3D view. At each point, the user can also change the parameters of the preprocessing step and re-run the analysis to achieve improved domain results. The user is also
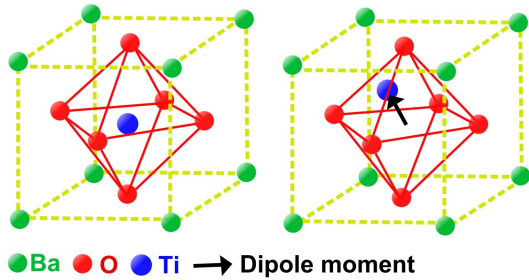
Figure 3: *Left: Barium titanate unit cell. Right: Titanium movement during phase transition used for dipole moment calculation.*

able to store videos of his data exploration or create animations including tracking shots or development over different time steps.

4   DATA PROCESSING STAGE

In order to achieve interactive frame rates during the interactive exploration and analysis the data has to be preprocessed. The dipole moments of all unit cells of the barium titanate grid have to be precomputed, and depending on these dipole moments the polarization domains have to be determined by clustering. In the following we will give a brief overview of both processing steps. Beside these two steps only the radar glyphs (see Sec. 5.1.3) have to be precomputed. Our method requires a total preprocessing time of nearly 1.5 minutes for a molecule grid with 50^3 unit cells and 500 time steps. If necessary, this step could be performed on-the-fly by leveraging a highly parallel computation framework as it has been done by Hawick et al. [7]. However, this approach would cause little delays during time step changes. Therefore, we have chosen to provide a delay free analysis stage by accumulating all calculations in one stage when a dataset is first loaded and caching the results.

4.1   Dipole moments

During the phase transition from the paraelectric to the ferroelectric phase, the initially unpolarized cubic unit cells should become tetragonal, and the displacement of the positively charged titanium atom and the centroid of the negatively charged oxygen octahedron should lead to a polarization. This behavior is illustrated in Fig. 3. Thus the first obvious attempt is to represent the dipole moments by the spatial displacement between the titanium atom and the octahedron centroid. This approach is not physically correct, since the dipole moment would take the exact partial valence charges of the ions into account, which are not always given by molecular dynamics. Nevertheless, since we are primarily interested in the direction of the polarization and not its magnitude, this simple calculation meets our requirements.

However, using our test dataset (see Sec. 6) revealed this method as not feasible. Caused by the molecular dynamics simulation and numerical inaccuracies the centroid of the oxygen octahedron fluctuates quite heavily between subsequent time steps. The dipole moment directions inherit this fluctuation. Therefore, domain structures cannot be detected this way.

To avoid the uncertainty of the positions of all seven atoms used in the calculation, we tried a second approach just considering the titanium atoms. By assuming an unpolarized stable configuration in the first time step of the simulation, the dipole moment direction can be quantified as the spatial difference between the titanium position in the first time step and the position in the current time step. This method was suggested by a domain expert and also used by Scharnowski et al. [20]. In the following we will use the term displacement equivalent to dipole moment.

Independent of the calculation method an averaging of atom positions through time steps can be done to filter deviations of these positions. The user can specify a time interval during which each atom's positions are averaged. Different weighting functions are offered such as Gaussian or uniform distributions. In our case a time interval covering about 20 time steps with a uniform distribution weighting delivers the best results. This again was suggested by a domain expert and also used in the application by Scharnowski et al. [20].

The dipol moment calculation takes nearly 30 seconds for a molecule grid with 50^3 unit cells over 500 time steps.

4.2   Domain detection

In order to detect polarization domains in the data, we employ a neighborhood detection scheme which focuses on the six immediate neighbors of each unit cell, based on the approach suggested by Pasćiak et al. [19]. The displacement direction of each cell is compared to its six neighbors along the positive and negative main axes by calculating the six scalar products between the current cell's and each neighbor cell's displacement. The user can specify a minimum scalar similarity threshold which determines whether or not a neighbor is considered similar to the current unit cell. The cell has a chance to become a seed of a domain if a user-defined condition is fulfilled: Either at least a specified number of individual neighbors are similar, or the average scalar product of all neighbors is greater than the similarity threshold. In our experience, a lower limit of at least three similar neighbors while using a similarity threshold of 0.85 delivered good results. If the condition is met, a region growing algorithm will search similar neighboring voxels in the same fashion to expand the seed to a full domain. If there are no more similar neighbors to expand the domain to, the algorithm checks if a minimum user-defined size of the

domain was reached. If this is the case, the domain is assigned a unique ID, and the algorithm continues with the remaining non-visited unit cells. Before assigning the ID, the algorithm checks the domain analysis result of the previous time step to check for domains with similar centers of mass and displacement direction as in the current result. If the distance between a previous and a current domain center of mass is below a user-defined threshold and the angle between the average displacement directions are below a user-defined angle, the domains are considered to be identical, and the new domain is assigned the corresponding old ID. Otherwise, a new ID which has not been used before is issued. This way, each domain ID occurs only once, and domains can be identified and tracked over the course of several time steps. The domain calculation takes, like the dipole moment calculation, nearly 30 seconds for a molecule grid with 50^3 unit cells over 500 time steps.

5 VISUAL ANALYSIS STAGE

The interactive visual exploration and analysis stage allows the user to choose between the *grid mode* and the *domain mode*. In the following we will describe the visualization techniques used in both modes. We will point out the special usage of each technique according to the specific task during the data exploration and outline implementation details.

5.1 Grid mode

The visual analysis stage will start in grid mode as shown in Fig. 2a to give the user an overview of the entire dataset. Initially the user will observe the bar plot located at the bottom of the application window which for each time step alternatively indicates the total number of molecules assigned to domains or the number of detected domains. This information gives the user a first impression when phase transitions might have taken place and which time steps could be interesting to analyze in detail. By clicking on a bar of the plot the corresponding time step will be loaded. The predecessor or successor time step can be loaded by clicking on the arrow buttons next to the plot as mentioned in Sec. 3.

Beside numerical parameters corresponding to the loaded time step, which are displayed on the right side of the tool window, the upper left 3D view visualizes the entire molecule grid or the displacements of each unit cell and thus enables a first approximate detection of polarization domains within the time step (see Sec 5.1.1). These potential domains can be explored in more detail in the three slice views as described in Sec. 5.1.2.

If the bar plot does not reveal any conspicuous time steps or the user does not want to focus on single ones, the radar glyph representation (Sec. 5.1.3) can be used to gain displacement information about the whole dataset.

#### 5.1.1 Molecule and displacement view

In grid mode, the user can choose between three visualizations in the 3D view, the *molecule representation*, the *displacement representation* and the *radar glyph representation*. Each representation will display information about the entire grid for the current time step, except the radar glyph representation (see Sec. 5.1.3 for details). The grid can be clipped along the main planes to reduce the visual clutter. In each representation the user can rotate and zoom the view using a trackball metaphor. The molecule representation provides a classic ball-and-stick model design, in which atoms are rendered as spheres and the electron bonds between atoms are rendered as cylinders (Fig. 4a). The color and size of each element can be changed by the user. To render nearly one million spheres and cylinders with interactive frame rates (30-40 fps), geometry shaders with billboard techniques [16] are used. As a result, the entire grid can be continuously displayed while using the trackball metaphor or switching between time steps.

The displacement representation shows arrows pointing along the corresponding dipole moment direction for each unit cell. The color of each arrow can be encoded in two ways. The first way encodes the length of the displacement, defined by a transfer function (TF) [4] chosen by the user. Visual clutter can be reduced by using the opacity value of the TF (Fig. 4b), which fades out arrows with small length. Assuming a higher magnitude of displacements of unit cells assigned to polarization domains, simple clusters can be detected in this representation. The second color encoding maps the displacement direction onto the color (see Fig. 4c), as it has been done by Grottel et al. [6]. As in the previous encoding the TF can be used to reduce the visual clutter by fading out small displacements. This time only the opacity value and not the color values of the TF are taken into account. The user can easily identify regions of the same displacement orientation. In both color encodings geometry shaders were used to provide a fluid visualization during navigation as in the molecule representation with approximately 50 fps.

The radar glyph representation shows 3D radar glyphs (see Sec. 5.1.3) for each unit cell. They use the same transfer function to obtain colors as the arrows of the displacement representation. The dipole moments of all unit cells over all time steps can be visualized in a single static image by this representation. During this representation the frame rate drops to a minimum 20 fps caused by the number of lines to render.
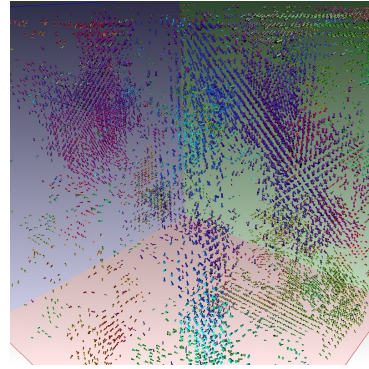
5.1.2 Similarity view

The three 2D slice views constitute the *similarity view* (Fig. 5), which can be used in both application modes
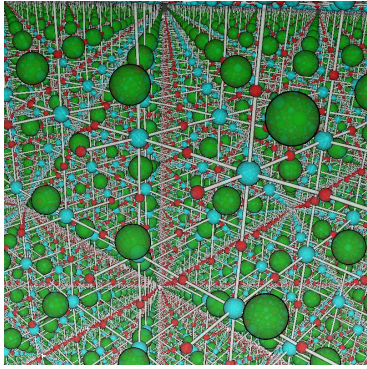
**(a)** *Classic ball-and-stick model of the barium titanate molecule grid in closeup.*
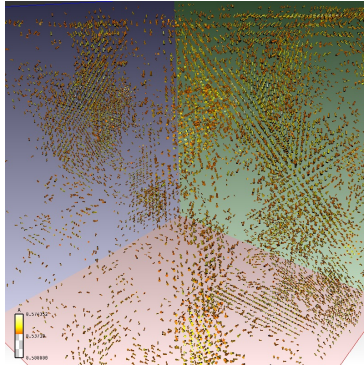
(b) *Representation of the dipole moments by a vector field colored by displacement length. Small displacements are clipped by transfer function.*
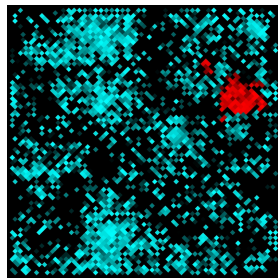
(c) *Representation of the dipole moments by a vector field colored by displacement direction. Small displacements are clipped by transfer function.*

Figure 4: *Different 3D visualizations of the entire molecule grid of a single time step.*
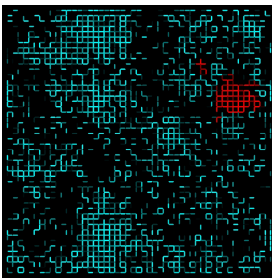
(a) *Digital layout of the 2D similarity view*

(b) *Diamond layout of the 2D similarity view*

Figure 5: *Example screenshots of the similarity view in both offered layouts (a)-(b). A selected domain in the domain mode is highlighted in red.*

(grid and domain mode). In each view, a slice through the dataset orthogonal to one main axis can be selected by scrolling through the dataset with the mouse wheel. In order to help the user navigate the three 2D slice views, each slice's current position is synchronized with a colored rectangle drawn in the 3D view (e. g., Fig. 9b), in which the color of the rectangle corresponds to the color of the slice border.

In the similarity view, the directional similarities between the displacement of each unit cell in the given slice and its immediate neighbors are depicted as colored 2D digital lines. Alternatively, for a more filling look, a diamond representation can be used (see Fig. 5b). The closer the directional similarity between neighbors is, the brighter the rendered object between them. This is achieved by mapping the scalar product of two neighboring normalized displacements to the opacity value of the color. Negative scalar products are mapped to zero, since they correspond to opposite displacement directions. Domains identified by unit cells with similar displacement directions are visualized as connected regions, while borders between domains with opposite directions will appear as gaps. This way, a user can already visually identify regions

with similar displacements in grid mode, without using the results of the domain analysis.

In domain mode, selected domains will be highlighted in these views (see Fig. 5). Thus it is possible for the user to align all slices to one selected domain and to detect imprecision in the domain detection.

Since the screen space is limited and the representation would become too small for increasing molecule grid dimensions, it is possible to shift the slice and zoom in to see regions of interest in more detail.
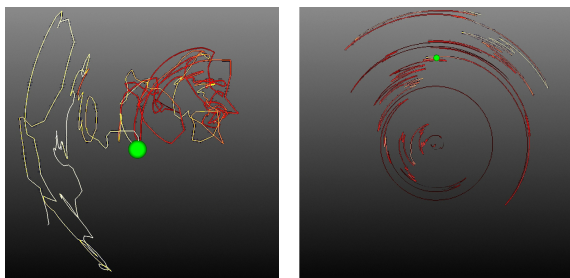
5.1.3 Radar glyph representation

The *radar glyph representation* was inspired by the work of Hlawatsch et al. [8]. The original (flow) radar glyphs were invented for flow visualizations. They are capable of representing the flow direction of one point in space over all time steps in one glyph. Hence, this technique allows the user to see the development of each unit cell's dipole moment displacement over all time steps in one single static image. The glyph's increasing radius represents increasing time, while the progression of the glyph-line plots the directional changes of the displacement vector like the glyph by Hlawatsch (see Fig. 6a). Since the original glyph just captures the direction of the flow and not the magnitude, the length of the displacement is color-mapped onto the glyph with a user-defined transfer function.

We provide this representation in 2D and 3D. A 3D glyph is shown in Fig. 6b. In this view it is hard to verify spatial directions without camera interaction. This problem does not occur in the case of 2D views, where a projection onto the plane that corresponds to the respective 2D slice has to be performed (Fig. 6 (c)-(e)). By rendering a green sphere into the glyph at the position corresponding to the currently loaded time step, the user gets a feedback which time steps are belonging to the glyph's part of interest. Furthermore, the spheres serve as a visual link between different radar glyph views.
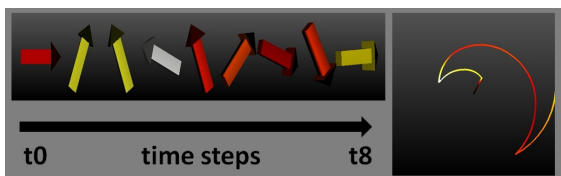
(a) *Mapping displacement directions over nine time steps onto a glyph. t0 is the center of the glyph. Increasing time is mapped onto increasing radius. Color and direction of displacements are not changed.*

(b) *3D example radar glyph of the test dataset.*

**(c)** *2D projection of the same glyph as in (b) onto XY-plane.*

Figure 6: *(a) illustrates the calculation of the radar glyphs. Color represents the length of the arrow. (b) is a 3D example of a glyph. Without camera interactions spatial directions are hard to verify. (c) is showing the glyph from (b) in 2D. The green sphere indicates the position of the same time step in each image.*

By considering more unit cells of the molecule grid, regions of similar displacement behavior will become visible in this representation mode (Fig. 10).

The glyphs were implemented with vertex buffer objects (VBOs) and geometry shaders to handle the large amount of vertices. The 3D view of a 50^3 unit cell dataset with 500 time steps, which has about 62.5 million line segments, can be rendered with an interactive frame rate (15-20 fps). However, the first calculation of the glyphs takes nearly 30 seconds and is done in the preprocessing stage (see Sec. 4). Afterwards the VBOs are cached and the calculation can be skipped during the next application start using the same input data.

5.2 Domain mode

After getting an overview of the simulation data in grid mode the user can switch to domain mode (see Fig. 2b). All views are now changing in order to display only regions of the grid which have been identified as polarization domains. The most important view is the *domain analysis view* which is located in the upper left and replaces the 3D molecule/displacement view of the grid mode. For more details on this view see the following Section 5.2.1. When selecting a domain of interest, which the user potentially has discovered in grid mode, numerical parameter values corresponding to this domain are shown on the right of the framework. They
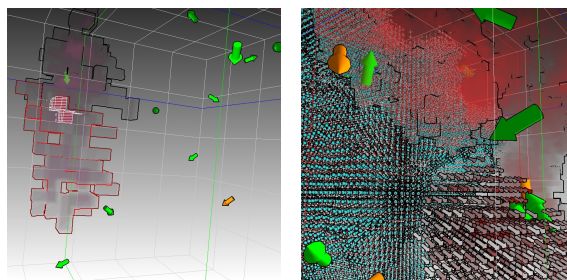
(a) *Domain analysis view showing detected domains glyphed by their average displacement direction. The common border between two domains in volume representation is highlighted.*

(b) *Domains visualized in different representations in one view. Left: Molecules, Right: Arrows, Top: Volumes.*

Figure 7: *Screenshots of the domain analysis view.*

include, for instance, the number of unit cells belonging to this domain as well as its lifetime, i.e., the interval determined by the time step it was detected first and the last time step it was found in the dataset. All values can also be plotted in a bar plot only showing the time steps of the domain's lifetime. Furthermore, a 3D radar glyph visualizes the average displacement of the domain and is linked to the domain analysis view. Rotation in the view will also effect the glyph, and displacement directions can be easily compared. Like in grid mode, the bar plot at the bottom can be used to navigate trough the time steps. The selected domain stays selected, which allows an observation of the evolution of the domain over its lifetime. This evolution can also be automatically animated to get a better understanding of the temporal and spatial extent of the domain.

The similarity view (Sec. 5.1.2) slightly changes in the domain mode. The selected domain will be highlighted as shown in Fig. 5. In this way, the three slices of each view can be adjusted to intersect the selected domain, and the user can get a feedback on the quality of the automatic detection and whether she has to restart the data processing stage with new parameters.

5.2.1 Domain analysis view

By switching to domain mode, the domain analysis view will replace the 3D view in grid mode. Its main purpose is to visualize the spatial interaction between domains in one time step and the temporal evolution of selected domains. Initially, each domain is displayed as a single arrow whose size corresponds to the number of unit cells of the respective domain. If a domain is added in the current time step, which has not been present before, the arrow will be displayed in orange color, otherwise it will be green (Fig. 7a). This way, new domains can be easily identified while browsing through the time steps. The user can now change the representation of each domain individually by right-clicking onto one of the arrows, which will open a context menu to specify the new viewing representation for the selected domain.
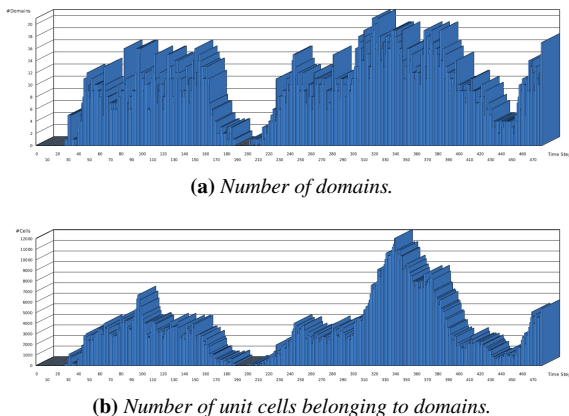
(a) *Number of domains.*

(b) *Number of unit cells belonging to domains.*

Figure 8: *Both plots showing the results of our test dataset.*

As long as the domain exists, its viewing mode will remain constant when changing time steps. The user can choose from the previously introduced molecule, arrow or radar glyph representations, which when selected now only show the unit cells belonging to the respective selected domain (Fig. 7b). Furthermore, each domain can be displayed using the *volume view*, which exploits GPU-based volume ray-casting [14] combined with image-space edge-detection (Fig. 7a). The necessary grid-sized volume dataset is generated by associating each unit cell with one voxel, and filling those areas of the volume dataset with a unique intensity value which corresponds to a specific volume view domain. In order to combine the geometry, e.g., arrows, with volume rendering, we have modified the exit points used by our ray-caster, which allows for correct geometry integration into the ray-casting process.

The volume representation provides the viewer with a better understanding of the extent of the selected domain, especially in context with neighboring domains. To allow the inspection of the border between two domains, we modified the ray-casting algorithm so that a common border between two domains in volume representation will be highlighted with a high-opacity color pattern. This provides the user with improved visual tracking of domain growth over time (Fig. 7a).

6 RESULTS

We used a molecular dynamics dataset provided by the IEEE VisWeek SciVis contest [23] to validate our system, since no other datasets were available to us. It contains a 50^3 barium titanate unit cell grid over 500 time steps. The MD simulates the ferroelectric phase transition caused by decreasing temperatures over a period of 10 nanoseconds, beginning in the paraelectric cubic phase.

Working with this dataset was not easy. The results were not expected in this way and differ from literature as also stated by Scharnowski et al.[20]. However,
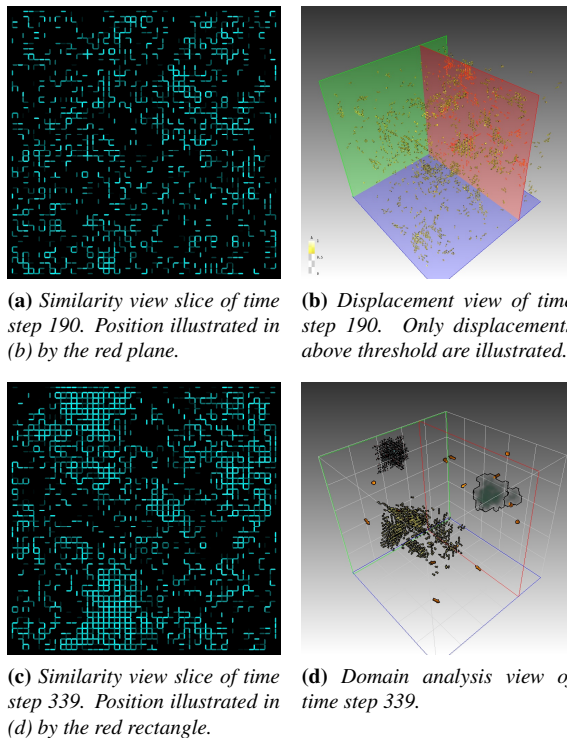

(a) *Similarity view slice of time step 190. Position illustrated in (b) by the red plane.*

(b) *Displacement view of time step 190. Only displacements above threshold are illustrated.*

(c) *Similarity view slice of time step 339. Position illustrated in (d) by the red rectangle.*

(d) *Domain analysis view of time step 339.*

Figure 9: *Different visualizations of time steps 190 and 339.*

here are our results:

A first result is illustrated in Fig. 8 showing both plots provided by our application. Significant in Fig. 8a is the lack of domains around time step 190. This is caused by strict parameters used in this study. Only potential domains with at least 120 unit cells are rated as domains. However, loosening the thresholds results in more detected domains in each time step, still having a local minimum at 190. On the other hand, we have a local maximum of unit cells belonging to domains around time step 339 (Fig 8b). Both time steps could indicate special moments of the phase transition.

Based on the first impressions of the plots we had a closer look at these time steps as illustrated in Fig. 9. The similarity view in Fig. 9a confirms the results of the plots. No larger regions of unit cells with higher similarity can be found. This is also visible in Fig. 9b showing the displacement view. Only a few displacements are pointing in the same direction.

The high density of domains in time step 339 can easily be found in Fig. 9c. As an example the domain analysis view of this time step is shown in Fig. 9d. It could now be used to observe the temporal evolution of single domains in detail.

Furthermore, the radar glyphs give insights into the temporal behavior of single unit cells. Figure 10 shows a part of a 2D slice of the YZ-plane located at row 15. Groups of neighboring cells having approximately the same displacement direction over the entire 500 time
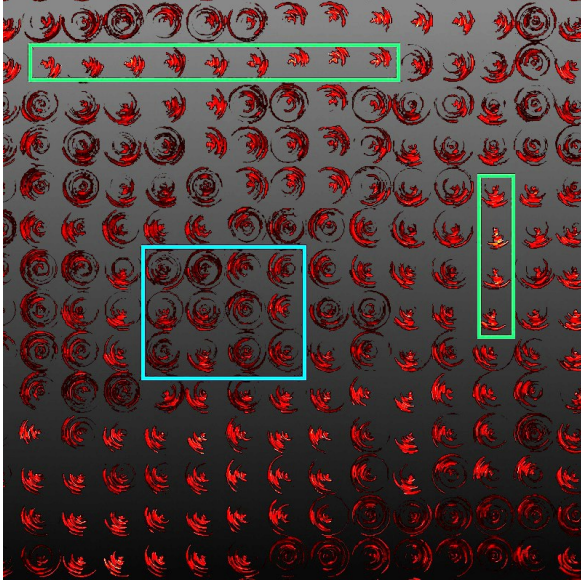
Figure 10: *2D glyph slice number 15 of YZ-plane. The green rectangles highlight two groups of unit cells with relatively constant directions, the blue rectangle highlights a group of unit cells with rotary directions.*

steps can be seen highlighted in green. Unit cells in the center (blue highlight) seem to have a more varying dipole moment indicated by the roundness of the glyphs. This challenges the theory of constant polarization domains and varying cells rated as domain borders. A deeper study of this behavior could be helpful.

7 FEEDBACK OF DOMAIN EXPERTS

We have demonstrated our system using the contest dataset [23] to seven researchers from different groups of physicists working in the field of materials science. Each of them immediately pointed to the domain plot and noted the physically impossible look of the plot. It should look more like a sign function with an impulsive rapid increase, followed by a constant high level of domains. After checking our calculations they agreed to our worries about the incorrectness of the MD we used. Unfortunately they could not provide us with new data, since they just do 2D simulations or 3D simulations with a 3^3 grid, which would be too small for our system. Therefore, during the further discussion they just focused on the visualization techniques with their potential usage and not on the physical correctness of the test dataset. However, this incident underlines the importance of the 2D plot as first step of the visual analysis. They all concurred with the main concept of one 3D view linked with three 2D views, since they are more used to 2D representations, but want to have a three dimensional feedback. The similarity view was considered as useful, but the switch between lines and diamonds as dispensable. The lines representation was considered as adequate and better looking than the

diamonds. The experts were skeptical about the use of the radar glyphs. However, two of them were interested to apply the glyphs to their 2D data and evaluate the use. Referring to the 3D view the arrow representation was considered as most useful, especially the possibility to simply fade out displacements with low amplitudes. The color mapping on directions was not implemented in the first design and has been added after the request of the experts. Nevertheless, they wanted to have both arrow color mappings.

Their overall conclusion was that our application is well designed and, in their opinion, contains high-end visualizations. However, it is two years too early to evaluate the entire capability of the system, since the scientific community is just moving from 2D to 3D simulations, resulting in a lack of a proper test dataset.

8 CONCLUSIONS

We have presented an interactive system for the analysis of phase transitions and polarization domain formation in ferroelectric materials. We provide proven molecule renderings as well as proven visualizations such as the 2D similarity view or the combination of geometry based and volume rendering based techniques. The performance of our system allows the user to exploit these rendering techniques while interactively switching between time steps.

The study of domain formation in barium titanate is still in a relatively early state. An iterative process could be established to advance this field of research. By using the visual results provided by our system, material scientists could derive improved mathematical frameworks describing the process. This would enable them to refine their numerical simulations and to draw new conclusions about the behavior of polarization domains. In turn, these findings could then be used to improve our framework, resulting in even more accurate visualizations.

Therefore, we are trying to establish a collaboration with materials science researchers to enhance our system. Since they can only provide 2D simulations at the moment, we will focus on developing 2D visualizations, which will be integrated into the system. Furthermore, it would also be interesting to extend the application to handle further ferroelectric materials with displacive phase transitions, which probably just affects the dipole moment calculation. Beside the highlighting of domains in all views, the domain experts recommended to highlight the border between neighboring domains in all views. This suggestion has not been implemented yet, but will be integrated in newer versions. Last but not least, additional numerical algorithms for the domain clustering could be implemented. Thus, the user could be further supported in detecting accurate polarization domains.

9 ACKNOWLEDGMENT

10 REFERENCES

[1] B. J. Alder and T. E. Wainwright. Studies in molecular dynamics. i. general method. *J. Chem. Phys.*, 31:459, 1959.

[2] S. Amelinckx and H. Blank. *Direct Observation of Ferroelectric Domains in Barium Titanate by Means of the Electron Microscope.* Euratom, 392. Euratom, 1963.

[3] Mike Carson and Charles E Bugg. Algorithm for ribbon models of proteins. *Journal of Molecular Graphics*, 4(2):121 – 122, 1986.

[4] Robert A Drebin, Loren Carpenter, and Pat Hanrahan. Volume rendering. In *ACM Siggraph Computer Graphics*, volume 22, pages 65–74. ACM, 1988.

[5] M. El Marssi, F. Le Marrec, I. A. Lukyanchuk, and M. G. Karkut. Ferroelectric transition in an epitaxial barium titanate thin film: Raman spectroscopy and x-ray diffraction study. *Journal of Applied Physics*, 94(5):3307 –3312, sep 2003.

[6] Sebastian Grottel, Philipp Beck, Christoph Müller, Guido Reina, Johannes Roth, Hans-Rainer Trebin, and Thomas Ertl. Visualization of electrostatic dipoles in molecular dynamics of metal oxides. *IEEE Trans. Vis. Comput. Graph.*, pages 2061–2068, 2012.

[7] K. A. Hawick, A. Leist, and D. P. Playne. Parallel Graph Component Labelling with GPUs and CUDA. *Parallel Computing*, 36(12):655–678, December 2010.

[8] M. Hlawatsch, P. Leube, W. Nowak, and D. Weiskopf. Flow radar glyphs – static visualization of unsteady flow with uncertainty. *Visualization and Computer Graphics, IEEE Transactions on*, 17(12):1949 –1958, Dec. 2011.

[9] W. Humphrey, A. Dalke, and K. Schulten. VMD: Visual molecular dynamics. *Journal of Molecular Graphics*, 14:33–38, 1996.

[10] Charles Loring Jackson. August wilhelm von hofmann. *Proceedings of the American Academy of Arts and Sciences*, 28:pp. 411–418, 1892.

[11] Oleg Kolosov, Alexei Gruverman, Jun Hatano, Koichiro Takahashi, and Hiroshi Tokumoto. Nanoscale visualization and control of ferroelectric domains by atomic force microscopy. *Phys. Rev. Lett.*, 74:4309–4312, May 1995.

[12] Michael Krone, Katrin Bidmon, and Thomas Ertl. Interactive visualization of molecular surface dynamics. *IEEE Trans. Vis. Comput. Graph.*, 15(6):1391–1398, 2009.

[13] Michael Krone, John E. Stone, Thomas Ertl, and Klaus Schulten. Fast visualization of gaussian density surfaces for molecular dynamics and particle system trajectories. In *EuroVis 2012 Short Papers*, volume 1, 2012.

[14] Jens Krüger and Rüdiger Westermann. Acceleration techniques for GPU-based volume rendering. In *Proceedings of IEEE Visualization*, pages 287–292, 2003.

[15] G. H. Kwei, A. C. Lawson, S. J. L. Billinge, and S.W Cheong. Structures of the ferroelectric phases of barium titanate. *The Journal of Physical Chemistry*, 97(10):2368–2377, 1993.

[16] O.D. Lampe, I. Viola, N. Reuter, and H. Hauser. Two-level approach to efficient visualization of protein dynamics. *IEEE Transactions on Visualization and Computer Graphics*, 13(6):1616–1623, 2007.

[17] MegaMol project website http://www.visus.uni-stuttgart.de/megamol/.

[18] Jennis Meyer-Spradow, Timo Ropinski, Jörg Mensmann, and Klaus H. Hinrichs. Voreen: A rapid-prototyping environment for ray-casting-based volume visualizations. *IEEE Computer Graphics and Applications (Applications Department)*, 29(6):6–13, Nov./Dec. 2009.

[19] Marek Pasćiak, Salah Eddine Boulfelfel, and Stefano Leoni. Polarized cluster dynamics at the paraelectric to ferroelectric phase transition in BaTiO3. *The Journal of Physical Chemistry B*, 114(49):16465–16470, 2010.

[20] Katrin Scharnowski, Michael Krone, Filip Sadlo, Philipp Beck, Johannes Roth, Hans-Rainer Trebin, and Thomas Ertl. 2012 ieee visualization contest winner: Visualizing polarization domains in barium titanate. *Computer Graphics and Applications, IEEE*, 33(5):9–17, 2013.

[21] E. Shi, C.R. Cho, M.S. Jang, S.Y. Jeong, and H.J. Kim. The formation mechanism of barium titanate thin film under hydrothermal conditions. *Journal of Materials Research*, 9:2914–2918, 1994.

[22] Alexander Stukowski. Visualization and analysis of atomistic simulation data with ovito-the open visualization tool. *Modelling and Simulation in Materials Science and Engineering*, 18(1):015012, 2010.

[23] VisWeek2012. Ieee scivis contest 2012, 2012. http://sciviscontest.visweek.org/2012/VisContest/Home.html.

[24] DavidC. Whitley. Van der waals surface graphs and molecular shape. *Journal of Mathematical Chemistry*, 23:377–397, 1998.

[25] B.M. Wul and I.M. Goldman. Dielectric constants of titanates of metals of the second group. *Compt. rend. Acad. sci. URSS*, 1945.